NEW RESULTS OF FERMI FEL1 EOS DIAGNOSTICS WITH FULL OPTICAL SYNCHRONIZATION

M. Veronese*, E. Allaria, P. Cinquegrana, E. Ferrari, F. Rossi, P. Sigalotti, C.Spezzani,
Elettra-Sincrotrone Trieste, Trieste, Italy

Abstract

The electro optical sampling diagnostics (EOS) of the FERMI FEL has been recently upgraded with a full optical synchronization of its dedicated femtosecond fiber laser to the ultra-stable optical pulsed timing system of FERMI. For this purpose a dual synchronization electronics has been developed and installed. It exploits a mixed error signal derived from both optical to electrical conversion and from second harmonic generation based optical phase detection. For this second part a new optical setup including a cross correlator has been installed. The operation of the EOS has greatly benefited from the upgrade. The arrival time measurements have been compared with the ones from the bunch arrival monitor diagnostics (BAM) showing very good agreement. This new setup has also allowed to improve the bunch profile measurement. Some examples of measurement with ZnTe and GaP are presented. Finally, usability and operator friendliness of the new setup are also discussed.

INTRODUCTION

FERMI is a seeded free electron laser (FEL) operating in the spectral range from VUV to soft x-rays. It is based on a SLAC/BLN/UCLA type RF-gun, and a normal conducting LINAC, currently operated at 1.2 GeV (up to 1.5 GeV). Longitudinal compression is provided by two magnetic chicanes BC1 and BC2 (respectively at 300 MeV and 600 MeV). The FEL has two undulator chains, namely FEL1 [1] and FEL2 [2]. The first, FEL1, is a single cascade HGHG seeded free electron laser designed to provide ultrashort radiation pulses with energies up to hundreds of micro joules per pulse in the wavelength range from 100 nm to 20 nm. The second, FEL2, is a double cascade seeded system designed to reach 4 nm at the shortest wavelength, implementing the fresh bunch technique. Optimization of a seeded FEL is a multi-parameter optimization process. To reach an optimal FEL emission several conditions have to be met. All information pertaining the time of arrival and the temporal profile of the electron bunch are of crucial importance. For this reason an electro optical sampling (EOS) diagnostics station has been installed at the entrance of both the FEL undulators chains. This paper is focused on the FEL1 EOS (see Fig. 1). This device in based on a fiber laser oscillator installed in the tunnel and exploits the spatial encoding scheme. The FEL1 EOS initial operational experience has been described in [3]. We made a major upgrade to the locking of the laser with a full optical synchronization setup and electronics with the aim of improving the time jitter performances of the FEL1 EOS.

* marco.veronese@elettra.eu

EXPERIMENTAL LAYOUT

The layout of FEL1 chain, in the undulator hall, is depicted in Fig. 1. In the figure the electron beam travels from left to right and its trajectory is depicted in black. The seed laser is depicted as a red flash. The modulator undulator (MOD) is in light blue while the dispersive section is in green and radiator (RAD) undulators are in violet. After the last radiator the electron beam is bent towards the main beam dump while the FEL radiation travels towards the experimental hall. The EOS diagnostic station is installed just upstream the modulator and is depicted in yellow in Fig. 1.

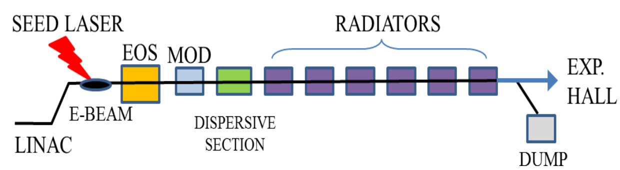

Figure 1: FERMI FEL1 layout.

The upgraded EOS optical layout is depicted in Fig. 2. The laser source is visible in the upper left part of the figure. It is a fiber laser (Menlosystems, TC780) delivering pulses at 780 nm wavelength with 110 fs duration, average power of 55 mW and repetition rate of 78.895 MHz. The pulses pass a delay line needed for fine time delay adjustments. Then the laser beam passes a Glan-Taylor polarizer (P) to improve polarization purity and a motorized zero order $\lambda/2$ waveplate for rotation of the polarization. The laser is focused on the electro optic (EO) crystals surface by a cylindrical lens (L2). The laser angle of incidence on the crystal is of 30 degrees with respect to the electron beam. This angle allows encoding temporal information in the spatial profile of the laser. After passing through the EO crystal the laser exits the vacuum chamber and passes through the polarization analysis optics. This is composed of two motorized waveplates ($\lambda/4$ and $\lambda/2$) and a Wollaston prism. They are adjusted to work in a cross polarizer configuration. The beam is then directed to the intensified charge-coupled device (ICCD) camera. Two lenses are set between the vacuum chamber and the ICCD camera to provide the necessary magnification. The vacuum 3-axis manipulator houses a ZnTe 1 mm thick crystal, a GaP 0.4 mm thick, a GaP 0.1 mm thick, an OTR screen and a YAG:Ce crystal. In the bottom part of Fig. 2 we show the coarse longitudinal alignment system. Coherent optical transition radiation (COTR) is used to set the correct ICCD gate delay. The extraction path for COTR radiation is depicted in violet.

ISBN 978-3-95450-141-0

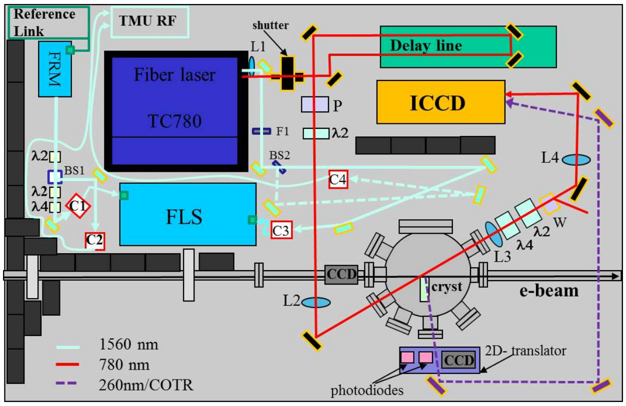

Figure 2: EOS optical table layout.

UPGRADES TO THE OPTICAL LAYOUT

To work as a time resolved diagnostics the EOS laser has to be phase locked to the pulsed optical timing system (OTS) of FERMI [4]. For this reason a dedicated phase reference fiber link for the EOS has been installed. The link delivers ultra stable pulses at 157.790 MHz with a wavelength of 1560 nm up to the end point of the link which is a Faraday rotator mirror unit (FRM). After the FRM the reference laser beam is in free space and it is split into and high power and a low power branches by a polarizing beam splitter (PBS). A $\lambda/2$ at the PBS entrance is used to control the power splitting ratio. The low power branch is fiber coupled by a collimator (C2) and used for RF locking. The high power branch is also fiber coupled via collimator (C1) and it is used for optical phase detection. The TC780 fiber laser is equipped with a secondary high power air output delivering 1560 nm pulses with a duration of about 350 fs. This beam is also split in two parts: one is used for optical phase detection (C3) while the other is sent via a fiber collimator (C4) to the locking electronics. The optical phase detection is performed via a Menlosystems fiber link stabilization (FLS) unit where the link and the reference pulses are cross correlated using a single crystal balanced detection scheme [5]. Both arms of the FLS have about 8 mW power on the second harmonic generation (SHG) crystal.

SYNCHRONIZATION ELECTRONICS

The optical equipment described above is used in a dual locking scheme where both RF locking and optical locking techniques are used at the same time. A layout of the synchronization electronics scheme is shown in Fig. 3. RF locking starts by converting laser and OTS link reference pulses to electrical signals extracting their common harmonics at 2.99801 GHz. Then the relative phase is detected by a heavily saturated RF mixer that produces a phase error signal which is used in the control loop. RF locking is very robust but does not give the needed performances in terms of time jitter and long term drifts. For this purpose optical locking in our case is added to RF locking. Both error signals from RF and optical phase detection are used for long term operation. The final proportional-integral (PI) controller is driven by weighting in the most efficient way RF and optical error signals. The control of the laser locking is achieved by two electronics units named TMU-RF and TMU-CU as described in [6]. This is the same electronics developed in-house for the synchronization of the FERMI photoinjector and seed femtosecond lasers. The TMU-RF

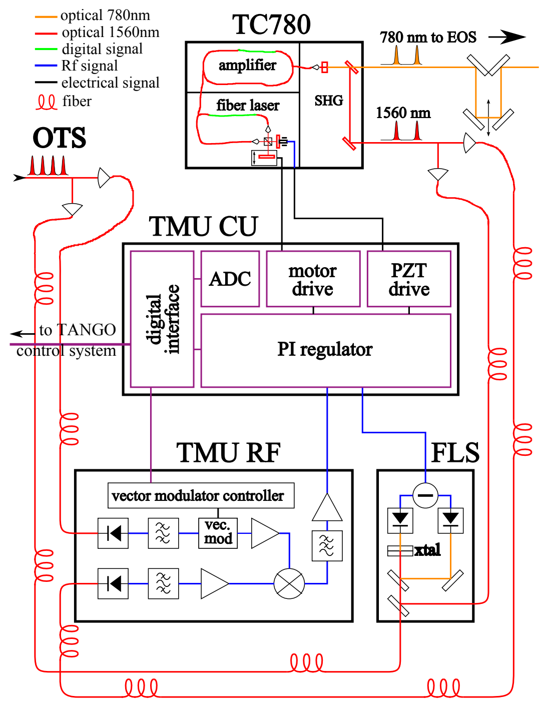

Figure 3: Synchronization scheme.

converts the optical signal from the fibers coming from either the link or the laser in RF signals. It performs a phase detection and generates an error signal which is fed to the TMU-CU. The TMU-CU controls the TC780 laser cavity stepper motor and piezo electric actuator to lock the phase of the laser to the reference link. Once this condition is reached the systems scans the time delay between laser and link to find the cross correlation position. This scan is done by deliberately changing the TC780 cavity frequency via a vector modulator acting on the RF converted signal from the laser while keeping it locked. The frequency difference causes a time slippage between the TC780 laser and the reference pulses. Once the cross correlation signal is found the delay is finely adjusted to reach the zero crossing. As a final step the PI loop controlling the locking is set to work at 80% based on the cross correlator signal reducing to 20% the weight of the RF error signal. The system is design to allow easy and remotely operated automatic synchronization of the laser. Moreover it provides all diagnostics information to the FERMI control system such as the optical power per each channel, the RF power per each channel, the error signal amplitudes, the 78.895 MHz and 2.99801 GHz phases as well as the frequency difference of the cavity, the cross correlator signal amplitude.

ISBN 978-3-95450-141-0

LABORATORY TEST RESULTS

One of the goals of this upgrade was to improve the time jitter of laser and thus of the EOS arrival time measurement previously at the level of 80 fs rms, by exploiting the full optical synchronization. The new synchronization system was tested in the laboratory. The TC780 laser was locked to an external optical master oscillator (Menlosystems TC1550 fiber laser), to establish the new system performances. The

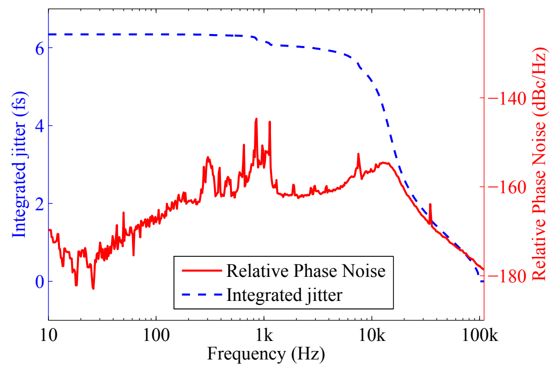

Figure 4: Phase noise data analysis of the TC780 laser locked to a TC1550 laser.

relative phase noise, measured in loop, is obtained from the output of cross- correlator, scaled by a conversion factor calculated from the cross- correlation signal slope. Data are acquired using a signal source analyzer (Agilent E5052B) used as a FFT analyzer. In Fig. 4 we show the measured phase noise curve in dBc/Hz (right axis and red solid curve) and the integrated jitter (left axis and blue dashed curve). The curve is then integrated up to 100 KHz which is the 3 dB cutoff limit of the bandwidth of the photodiode used in the cross-correlator. The total time jitter is of about 6 fs rms. After installation in the FERMI tunnel we performed again the phase noise measurement but this time with the laser locked to the stabilized pulsed fiber link. When locked to the reference fiber link the phase noise is the same within the error of the measurement which is about ±10%.

E-BEAM ARRIVAL TIME MEASUREMENTS

The performances of the EOS diagnostics after the described upgrade of the synchronization system have been tested on the electron beam of FERMI. We deliberately caused a change of arrival time of the electron bunch by modifying in a controlled way the electron trajectory in the first bunch compressor. During this operation we recorded shot by shot the bunch arrival time with the EOS and for comparison with the nearby bunch arrival monitor (BAM). An example of this kind of measurement is shown in Fig. 5. In this case we induced a modulation of the arrival time of about ± 400 fs and recorded the EOS and BAM measurements for the same FERMI electron bunch. In the upper plot, the horizontal axis of the figure is the FERMI bunch

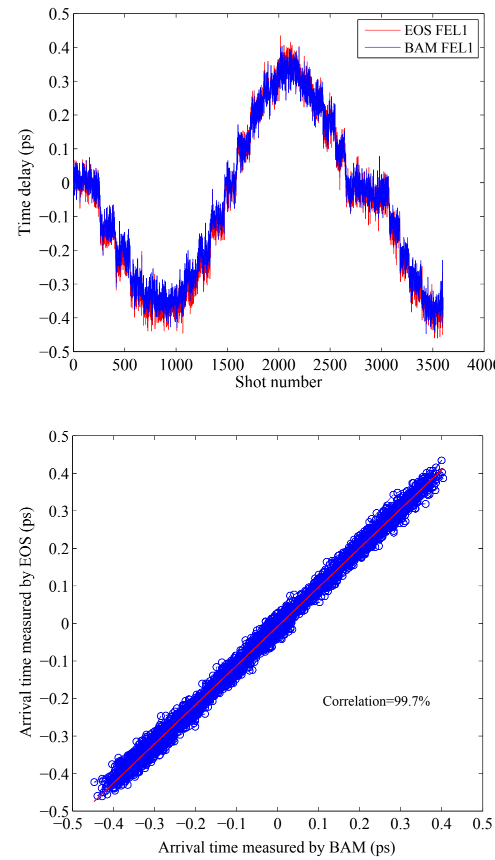

Figure 5: Upper plot EOS (red) and BAM (blue) arrival time vs bunch number. In the bottom plot we show EOS arrival time vs BAM arrival time.

number while on the vertical axis we have the time of arrival measurement performed with the BAM and the EOS. The data are plotted one versus the other in the lower plot an their correlation is of 99.7%.

PROFILE MEASUREMENTS

As described before, the EOS manipulator is equipped with three electro optic crystals: ZnTe 1mm thick, GaP 0.4mm thick and GaP 0.1mm thick. The ZnTe crystal is protected with a fused silica optical substrate coated with an high reflectivity coating to protect it from the seed laser in the event of a wrong steering. Since GaP has a higher damage threshold than ZnTe, no protection is installed. The ZnTe has a higher EO coefficients and thickness, thus single shot bunch profiles can easily be acquired. In Fig. 6 we present a typical sequence of profiles acquired at 10 Hz. In the figure the profiles are stacked adding an offset to improve image quality. The centroid position for each bunch is calculated and the rms deviation is the bunch arrival time jitter, typically of about 40 fs. The ZnTe offers the best signal to noise ratio but the temporal resolution is insufficient for accurate bunch profile measurements. For sub picosecond electron bunch profile measurements the best resolution in

ISBN 978-3-95450-141-0

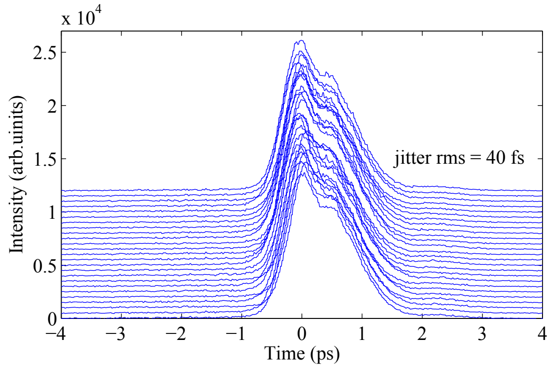

Figure 6: EO signal of 30 consecutive bunches (ZnTe).

FERMI EOS is obtained with the GaP 0.1 mm crystal because of its better frequency response and smaller thickness. The lower electro optic coefficient of GaP compared to ZnTe and the reduced thickness produce a lower rotation of the polarization. This means a lower EOS signal which of the same order of magnitude of the background and optimization of the waveplates is needed to maximize SNR. Also a subtraction of the background (unrotated polarization) is needed to obtain a bunch profile with no artifacts. As an example we show in Fig. 7 an EOS profile measurement with the GaP 0.1 mm thick, after background subtraction. In the figure we also show an asymmetric Gaussian fit of the profile. The FWHM of the profile is of about 1.15 ps but the profile sides have different slopes. The left side is much steeper and has a Gaussian sigma of 154 fs. All the

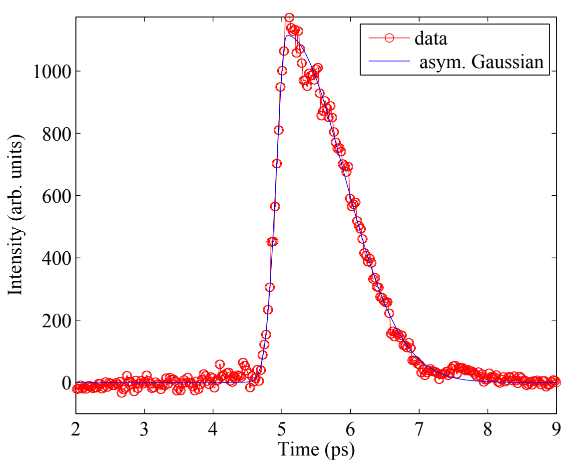

Figure 7: Bunch profile acquired with the GaP 0.1 mm crystal (in red) and asymmetric Gaussian fit (in blue).

information provided so far are based on a calibration of the temporal scale which converts ICCD pixels to picoseconds. The time calibration of the EOS for spatial encoding is usually performed comparing the transverse rms beam size of the laser on the crystal (σ_C) and the transverse rms beam size of the laser on the ICCD (σ_{ICCD}). For a given angle α between the electron beam and the laser propagation direction, the equivalent temporal sigma is defined as $\sigma_t = \sigma_C * \cos(\alpha)/c$ where c is the speed of light in the vacuum [7]. Knowing σ_t, the pixel to picosecond conversion is determined. The new ultra stable synchronization system has allowed us to devise another way to calibrate the EOS by scanning the position of the delay line while recording the beam profiles. Averaging over multiple shots we reduce the effect of the already small time jitter over the determination of the average e-beam temporal arrival time and in this way a direct time to pixel conversion can be performed. Both calibration methods have been tested. The first gives a calibration constant of 73 px/ps while the second 77 px/ps, in both cases an error from 5% to 10% is to be expected. In conclusion, we have installed a dual synchronization system that has greatly enhanced the usability and eased the operation of the EOS as well as allowed time of arrival jitter measurements with an accuracy level comparable to the one of the BAM. Also the profile measurements have benefited from the upgrade. We reported on the resolution of profile measurements, showing a value below 150 fs.

REFERENCES

[1] E. Allaria et al., “Highly coherent and stable pulses from the FERMI seeded free-electron laser in the extreme ultraviolet”, Nature Photonics, 6, 699, (2012).

[2] E. Allaria et al., “Two-stage seeded soft-X-ray free-electron laser”, Nature Photonics 7, 913, (2013)

[3] M.Veronese et al.,“First operation of the electro optical sampling diagnostics of the FERMI@Elettra FEL”, Proc. IBIC2012, Tsukuba, Japan, pp. 449, (2012).

[4] M. Ferianis et al. “All-optical femtosecond timing system for the FERMI@Elettra FEL.”, Proc. FEL2011, Shanghai, China, pp. 641, (2011).

[5] J. Kim et al., “Long-term femtosecond timing link stabilization using a single-crystal balanced cross correlator”, Optics Letters 32, 1044 (2007).

[6] P. Sigalotti, et al., “Ultrafast laser synchronization at the FERMI@Elettra FEL”, Proc. SPIE 8778, Advances in X-ray Free-Electron Lasers II: Instrumentation, 87780Q, (2013).

[7] A.L. Cavalieri, Ph.D. thesis, The University of Michigan, (2005).

ISBN 978-3-95450-141-0